Supporting Information

Yan et al. 10.1073/pnas.1222285110

SI Materials and Methods

Clinical Evaluation. This study was approved by the Institutional Review Boards of the University of Miami (protocol 2001-0415), University of Washington (protocol 33468), and PLA General Hospital, Beijing. Informed consent was obtained from each adult subject and from a parent of each subject under age 18 y. Clinical history interviews, physical examinations, and audiometric evaluations were carried out as described previously (1). Air conduction thresholds were measured at 250, 500, 1,000, 2,000, 4,000, 6,000, and 8,000 Hz, and bone conduction thresholds were determined. All subjects were examined otoscopically, and oto-immittance measurements were obtained to assess middle ear status. Motor development history interviews and Romberg testing were performed to evaluate vestibular function. Subjects were asked to report noise exposure from age 12 y as either significant exposure to impulse noise (e.g., explosions in mining industries), high-level occupational noise (e.g., chronic loud noises in construction work), or neither. Subjects under age 13 y were excluded from assessment of the effect of noise on hearing, and exposures to impulse noise and occupational noise were combined. Peripheral blood samples were collected, and DNA was extracted according to standard methods.

Targeted Capture and Sequencing. A total of 3,636 cRNA 120-mer overlapping probes were designed to capture the 4.80-MB region spanning chr12:129,051,849-133,851,894 (hg19) that defines the DFNA41 linkage interval. The design included all 427 documented RefSeq, UniProt, and CCDS exons and flanking intronic splice sites (http://genome.ucsc.edu). Using the SureSelect Target Enrichment system (Agilent), 3 µg of DNA extracted from each subject's blood was sonicated to a peak of 150 bp and hybridized to the design. Sequencing was performed with 2×10^{-1} -bp paired end reads using SBS v3 on a HiSeq (Illumina) to a median read depth of 350×, with 99.2% of the targeted regions covered by a minimum of 10 reads. DNA variants were filtered against common polymorphisms documented by dbSNP135 or the National Heart, Lung, and Blood Institute's Exome Sequencing Project (http://evs.gs.washington.edu/EVS/). Rare and private variants were classified by predicted function as missense, nonsense, frameshift, or splice-site alleles. Variants were validated and tested for cosegregation with deafness in the family by Sanger sequencing using established methods.

Expression Plasmids. P2RX2 cDNA (NM_174873) in pCMV6-AC-mGFP (monomeric GFP) vector was obtained from Origene. P2RX2 p.V60L (c.178G > T) was introduced using the Quik-Change Mutagenesis Kit (Stratagene) according to the manufacturer's instructions.

Rat Inner Ear Tissue Cultures and *P2RX2* **Transfection.** Organ of Corti and vestibular sensory organs were dissected from postnatal day 2 (P2) rats in accordance with National Institutes of Health guidelines (protocol 1215-08) and maintained for 2 d in culture, then transfected with GFP-*P2RX2* WT or P2RX2 p.V60L using a Helios GeneGun (BioRad), as described previously (2). After 9 h, samples were fixed, permeabilized, and counterstained with Alexa Fluor 568 phalloidin (0.001 U/µL; Invitrogen). Efficiency of transfection ranged from 0 to 10 hair cells per explant. At least 20 transfected cells for each construct were examined by fluorescence confocal imaging.

Patch-Clamp Analysis of ATP-Evoked Current. Human embryonic kidney 293 (HEK293) cells were cultured in DMEM with 10% FBS and 100 U/mL penicillin at 37 °C in a 5% CO₂ incubator. At 90% confluence, cells were passed by trypsin-EDTA, reseeded at a 24-well plate with a density of 100,000 cells per well, and incubated overnight. The medium was then replaced with the fresh DMEM plus 10% FBS and a transfection reaction mixture containing OPTI-MEM medium, Lipofectamine 2000, and the *P2RX2* plasmid (WT or mutant). After 24–48 h, successful transfectants were identified under fluorescent microscopy. Cells were then trypsinized and replated with normal extracellular solution (130 mM NaCl, 5 mM KCl, 1.47 mM MgCl₂, 2 mM CaCl₂, 25 mM dextrose, and 10 mM Hepes; 300 mOsm, pH 7.2) in 35-mm culture dishes for whole-cell patch clamp recordings.

Single, isolated transfected HEK293 cells with strong fluorescence were selected, and whole-cell recording was performed with an Axopatch 200B patch clamp amplifier (Molecular Devices) (3–5). Patch pipettes were filled with an intracellular solution containing 140 mM KCl, 5 mM EDTA, 2 mM MgCl₂, and 10 mM Hepes (pH 7.2), with an initial resistance of 2.5–3.5 M Ω in bath solution. Data were collected with jClamp (SciSoft). The signal was filtered through a four-pole low-pass Bessel filter with a cutoff frequency of 2 kHz and digitized using a Digidata 1322A (Molecular Devices). Data were analyzed with jClamp and plotted using SigmaPlot software (SPSS), with bars representing SEs.

Measurement of FM1-43 Permeability Through P2RX₂ Channels. MDCK-II cells were plated on coverslips in a six-well plate and cultured as described previously (6). Well-polarized MDCK-II cells were transfected with 3 µg of GFP-P2RX2 WT or P2RX2 p.V60L, or with 1.5 µg of each construct simultaneously using 10 µL of GeneGuice transfection reagent (Novagen) per 35-mm well, and incubated for up to 48 h. Transfected cells were incubated at room temperature in 300 µM ATP (Sigma-Aldrich) in Leibovitz medium (Gibco) for 1 min, applied to 5 µM FM1-43 FX (Invitrogen) for 3 min, and washed twice with 500 µM Advasep-7 (Sigma-Aldrich) in PBS to reduce the background. Samples were fixed, permeabilized, and counterstained with Alexa Fluor 647 phalloidin. Both GFP and FM1-43 were excited by a 488-nm laser and detected by separate emission filters (PerkinElmer), 527 nm (W55) for GFP and 615 nm (W70) for FM1-43. FM1-43 FX emits at a different wavelength than GFP. Both are excited with the same wavelength, and the emitted fluorescence was collected using different filters. Fluorescence was quantified using ImageJ software.

Cells were scanned for FM1-43 dye using the same scanning parameters for all preparations, after which a contour was traced around each cell and total emitted fluorescence was extrapolated. For each condition, more than 20 cells were measured, and the average fluorescence per cell was calculated. All measures were normalized to emitted fluorescence from WT *P2RX2*.

Animals. All experiments were approved by the Animal Care and Ethics Committee of the University of New South Wales. *P2RX2*-null mice (B6.129-P2rx2tm1Ckn/J; Jackson Laboratory) (7) and background-strain C57BL/6J WT mice were born and raised in either an acoustically attenuated (quiet) environmental chamber or an environmental chamber with a continuous noise level of 75 dB SPL, 8–16 kHz. Both *P2RX2*-null and C57BL/6J mice (Jackson Laboratory) were rederived and bred at the transgenic facility of the University of New South Wales (Australian Bio-Resources). The background strain C57BL/6J is a model for

accelerated age-related hearing loss arising in part from a mutation in cadherin 23 ($Cdh23^{ahl}$).

Environmental chambers were custom-built with high acoustic attenuation, controlled ventilation, and a 12:12-h light:dark cycle. Each chamber housed up to 15 mouse cages with daily monitoring. The noise level in each cage was checked periodically with an acoustic spectral analyzer (Brüel Kjær) and a 1/2-inch microphone on an extension lead. In the "noise" chamber, two speakers (Altronic) were positioned over each cage to generate continuous filtered white noise (75 dB SPL, 8–16 kHz; second-order Bessel filter, 12-dB/octave dropoff). The noise was generated by custom software and a computer interface D/A converter (National Instruments) driving an audio amplifier (Altronic). The cages in the quiet chamber had a background noise floor of <8 dB SPL above 2 kHz.

Hearing Assessment in Mice. Assessments of hearing function by auditory brainstem response (ABR) and by otoacoustic emission (DPOAE) were performed using established protocols (8). Sound stimulation and response measurements (TDT III system; Tucker-Davis Technologies) of anesthetized mice were performed in an anechoic chamber (Sonora Technology). Puretone pips (5 ms; 4-36 kHz) or clicks (100 µs) were generated by a closed-field electrostatic speaker (EC1; Tucker-Davis Technologies). ABRs were recorded with fine platinum subdermal electrodes placed at the mastoid region of the stimulated ear (active electrode), scalp vertex (reference), and hind leg (ground). The intensity of the tonepips or click stimuli were reduced in 5-dB steps starting from 85 dB SPL to 10 dB below the threshold level where the ABR waveform was lost (up to 512 sweeps; threshold visibly determined within 2.5 dB). DPOAE assesses outer hair cell response to sound stimuli. Two EC1 speakers generated the primary tones (f_2/f_1 ratio, 1.25; 6–32 kHz from 0 to 70 dB in 5-dB steps), and otoacoustic emissions were detected by an ER-10B⁺ microphone (Etymotic Research).

- 1. Yan D, et al. (2005) Refinement of the DFNA41 locus and candidate genes analysis. J Hum Genet 50(10):516–522.
- Salles FT, et al. (2009) Myosin Illa boosts elongation of stereocilia by transporting espin 1 to the plus ends of actin filaments. Nat Cell Biol 11(4):443–450.
- Zhao HB, Yu N, Fleming CR (2005) Gap junctional hemichannel-mediated ATP release and hearing controls in the inner ear. Proc Natl Acad Sci USA 102(51):18724–18729.
- 4. Zhu Y, Zhao HB (2010) ATP-mediated potassium recycling in the cochlear supporting cells. *Purinergic Signal* 6(2):221–229.
- Yu N, Zhao HB (2008) ATP activates P2x receptors and requires extracellular Ca(++) participation to modify outer hair cell nonlinear capacitance. *Pflugers Arch* 457(2): 453–461.

Immunolabeling. Cochlear tissues from the quiet-raised 17-mo-old P2RX2-null and WT mice were examined by immunofluorescence confocal microscopy. Mid-modiolar cochlear cyrosections (40 µm) were prepared as described previously (9), permeabilized and blocked, incubated overnight in polyclonal rabbit anti-bovine antibody against 200-kDa neurofilament heavy (NF-200, 1:1,000; Sigma-Aldrich N-4142), and detected with Alexa Fluor 488 goat anti-rabbit IgG secondary antibodies (1:750; Life Technologies). The tissues were counterstained with rodamine-phalloidin conjugate (1:250; Life Technologies) and mounted onto slides in Pro-Long Gold Antifade Reagent with DAPI. No primary or primary/ secondary controls were included to determine the background signal level caused by secondary antibody labeling and autofluorescence. Images were acquired using a Zeiss Z1 AxioExaminer NL0710 confocal microscope with Zen 2008 software, with W/Plan-APO Chromat 20×/10× objectives, fluorescence detected by 488 nm ex/ 517 \pm 25 nm em (NF-200), 561 nm ex/ 618 \pm 53 nm em (phalloidin), and 790 nm two-photon ex/ 443 \pm 54 nm em (DAPI).

Statistical Analysis. The two-point LOD score for linkage of hearing loss to $P2RX2 \ c.178G > T$ in the DFNA41 family was calculated using MLINK (10), under a recessive model of full penetrance, no phenocopies, and a disease allele frequency of 0.001. All affected individuals and unaffected individuals age 20 and older were included in the linkage analysis. Hearing losses in noise-exposed vs. unexposed DFNA41 family members were compared by ranked two-way ANOVA. Hearing thresholds of WT and mutant mice raised in quiet vs. noisy environments were compared by two-way ANOVA with Holm–Sidak multiple pairwise post hoc comparisons. FM1-43 signal intensities, reflecting permeability of WT vs. mutant transfected MDCK-II cells, were compared using Tukey–Cramer tests. All tests were two-tailed.

- Grati M, Kachar B (2011) Myosin VIIa and sans localization at stereocilia upper tip-link density implicates these Usher syndrome proteins in mechanotransduction. Proc Natl Acad Sci USA 108(28):11476–11481.
- 7. Jiang LH, et al. (2003) Subunit arrangement in P2X receptors. J Neurosci 23(26):8903-8910.
- Cederholm JM, et al. (2012) Differential actions of isoflurane and ketamine-based anaesthetics on cochlear function in the mouse. *Hear Res* 292(1-2):71–79.
- Wong AC, Velamoor S, Skelton MR, Thorne PR, Vlajkovic SM (2012) Expression and distribution of creatine transporter and creatine kinase (brain isoform) in developing and mature rat cochlear tissues. *Histochem Cell Biol* 137(5):599–613.
- Lathrop GM, Lalouel JM, Julier C, Ott J (1984) Strategies for multilocus linkage analysis in humans. Proc Natl Acad Sci USA 81(11):3443–3446.

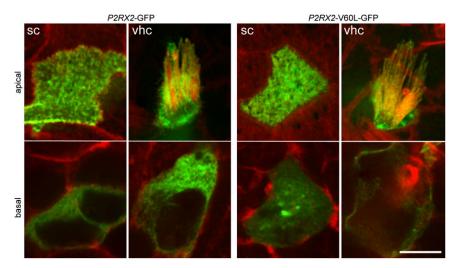


Fig. S1. Localization of $P2X_2$ receptors in rat vestibular hair cells and supporting cells. Both WT and mutant $P2X_2$ receptors preferentially target the plasma membranes of hair cells and support cells. Fluorescence confocal optical sections of rat vestibular tissue culture are shown, with GFP-tagged *P2RX2* WT and mutant constructs stained in green and actin counterstained in red. Images are of the hair cell and support cell apical surfaces and 7–8 μ m deep through the basolateral pole of the cell body. (Scale bar: 5 μ m.)

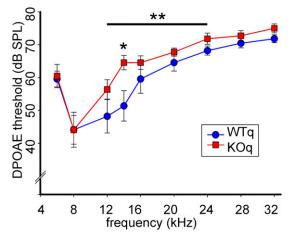


Fig. 52. DPOAE analysis of age-related hearing loss in *P2RX2*-null and WT mice raised in quiet. The quiet chamber was acoustically isolated, with background noise <8 dB SPL above 2 kHz. At 17 mo, *P2RX2*-null mice (n = 12) had significantly higher cubic DPOAE thresholds than WT mice (n = 8) in the 12- to 24-kHz range (P = 0.008).

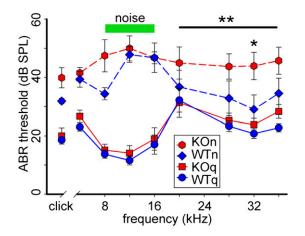


Fig. S3. Hearing of *P2RX2*-null and WT mice, age 19–23 wk, raised in quiet vs. noisy environments. Chronic exposure to moderate noise resulted in hearing loss at 8–16 kHz for both WT mice (WTn; n = 7) and *P2RX2*-null mice (Kon; n = 8). Hearing loss of the *P2RX2*-null mice vs. WT mice at 20–36 kHz was exacerbated compared with hearing loss at age 11–15 wk (P = 0.002) (Fig. 5*B*). In contrast, in the quiet chamber, *P2RX2*-null mice (KOq) and WT mice (WTq) had similar low thresholds and retained a clear demarcation of the best hearing sensitivity at 8–16 kHz. For both WT and *P2RX2*-null mice, the modest hearing losses at 20–36 kHz compared with age 11–15 wk may reflect progressive hearing loss associated with the mutation of *Cdh23* (1) on the background C57BL/6J strain (P = 0.16 for comparison with data of Fig. 5*B*).

1. Noben-Trauth K, Zheng QY, Johnson KR (2003) Association of cadherin 23 with polygenic inheritance and genetic modification of sensorineural hearing loss. Nat Genet 35(1):21–23.

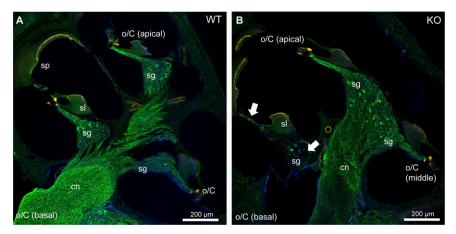


Fig. S4. Mid-modiolar confocal fluorescence images of cryosections of cochleae from 17-mo-old WT and *P2RX2*-null mice raised in quiet. Hair cells were labeled with rhodamine-phalloidin for filamentous actin (red). Spiral ganglion neurons and their central and peripheral processes were immunolabeled for neurofilament 200K (green). Cell nuclei were labeled with DAPI (blue). o/C, organ of Corti; sp, spiral prominence; sl, spiral limbus; sg, spiral ganglion; cn, cochlear nerve. (A) WT mice. (B) *P2RX2*-null mice. Note the degeneration of the sensory epithelium (organ of Corti), associated with loss of spiral ganglion neuron somata (arrows).